

## Multiparty multilevel energy-time entanglement

Giuseppe Vallone,<sup>1,2,\*</sup> Paolo Mataloni,<sup>2,3,\*</sup> and Adán Cabello<sup>4,†</sup><sup>1</sup>*Museo Storico della Fisica e Centro Studi e Ricerche Enrico Fermi, Via Panisperna 89/A, Compendio del Viminale, Roma I-00184, Italy*<sup>2</sup>*Dipartimento di Fisica, Università Sapienza di Roma, Piazzale Aldo Moro 5, I-00185 Roma, Italy*<sup>3</sup>*Istituto Nazionale di Ottica Applicata (INO-CNR), L.go E. Fermi 6, I-50125 Florence, Italy*<sup>4</sup>*Departamento de Física Aplicada II, Universidad de Sevilla, E-41012 Sevilla, Spain*

(Received 23 December 2009; published 5 March 2010)

Franson-like setups are inadequate for multiparty Bell experiments with energy-time entanglement because postselected events can depend on the local settings, and local models can exploit this feature to reproduce the quantum predictions, even in the case of ideal devices. We extend a previously introduced interferometric scheme [A. Cabello *et al.*, Phys. Rev. Lett. **102**, 040401 (2009)] to solve this problem in the  $N$ -qubit and  $N$ -qubit cases. In addition, the proposed setups allow us to prepare and test  $N$ -qubit Greenberger-Horne-Zeilinger and  $(\sum_{i=1}^N |i \cdots i\rangle)/\sqrt{N}$  energy-time entangled states.

DOI: [10.1103/PhysRevA.81.032105](https://doi.org/10.1103/PhysRevA.81.032105)

PACS number(s): 03.65.Ud, 03.67.Mn, 42.50.Xa, 42.65.Lm

### I. INTRODUCTION

Franson [1] showed how the essential uncertainty in the time of emission of a pair of particles can be exploited to make undistinguishable two alternative paths that the particles can take and create what is called “energy-time” or “time-bin” [2] entanglement, depending on the method used to have uncertainty in the time of emission. Franson proposed an experiment to demonstrate the violation of the Bell Clauser-Horne-Shimony-Holt (CHSH) inequality [3] using energy-time entanglement. However, Aerts *et al.* [4] (see also Ref. [5]) showed that, even in the ideal case of perfect preparation and perfect detection efficiency, there are local hidden-variable (HV) models that reproduce the quantum predictions for Franson’s test of the Bell-CHSH inequality. The reason is that, in Franson’s setup, the fact that photons are detected in coincidence can depend on the local settings. This can be exploited to build local HV models which simulate the quantum predictions (see Refs. [4,5] for details).

Recently [6], Franson has argued that these local HV models are not realistic in the sense of Einstein, Podolsky, and Rosen (EPR) [7], because they do not describe the path taken by the photons. However, in the Franson Bell-CHSH experiment, the path taken by one photon cannot be predicted with certainty from a measurement on the distant photon, thus the path is not an element of reality in the sense of EPR. The assumption that the local models must describe the paths taken by the photons is an extra assumption which is not necessarily satisfied by all local HV models. Actually, this extra assumption is equivalent to the extra assumption that the fact that a photon is detected at a specific time is independent of the local experiment performed on that photon. The introduction of this assumption was previously suggested in Ref. [4] as a way to avoid the problem. The Franson Bell-CHSH experiment can rule out local HV with this extra assumption but cannot rule out local HV models without this assumption.

Three different strategies have been proposed to solve this problem. Aerts *et al.* [4] proved that local HV models can be ruled out using a Franson’s setup with a very fast local switching if, instead of testing the standard two-setting Bell-CHSH inequality, a specific three-setting Bell inequality is tested. This solution has two problems: it requires a fast switching that is very difficult to achieve and also requires obtaining experimentally a violation which is very close to the maximum quantum violation obtained assuming ideal equipment (i.e., it requires nearly perfect visibility). To our knowledge, so far there is no experimental implementation of this proposal.

Brendel *et al.* [2] proposed a modification of Franson’s setup which, in principle, solves the problem. The modification consists of replacing the two beam splitters which are closer to the source by switchers synchronized with the source. However, to our knowledge, these active switchers are not available for photonic sources, thus in actual experiments they are replaced by passive beam splitters (see, e.g., Ref. [2]), so the resulting setup suffers from the same problem the original Franson’s setup has. Recently, it has been pointed out that active switchers could be feasible if photons are replaced by molecules [8].

More recently [5], we have proposed a more radical modification of Franson’s setup which solves the problem and can be actually implemented in the laboratory with photons. In our scheme, both the short path of the first (second) particle and the long path of the second (first) particle ends in Alice’s (Bob’s) detectors. Then, the selection of events is local (i.e., it does not require communication between Alice and Bob), since coincidences occur every time the local observer detects only one particle and, more importantly, is independent of the local settings (see the details in Ref. [5]). Due to this last property, this scheme does not suffer from the postselection loophole that affects *all* previous Bell-CHSH experiments with energy-time or time-bin entangled photons. This scheme has been recently implemented in the laboratory [9] and has inspired a new source of electronic entanglement [10].

The aim of this article is to extend this scheme to the multipartite case and discuss its applications for testing an important class of multipartite Bell inequalities using

\*<http://quantumoptics.phys.uniroma1.it/>†[adan@us.es](mailto:adan@us.es)

energy-time entanglement and preparing some multipartite multilevel energy-time entangled states relevant for quantum information processing.

The article is organized as follows. In Sec. II, we show that some previously proposed multipartite Franson-like configurations are inadequate for testing multipartite Bell inequalities of Mermin's type [11] with energy-time (and time-bin) entanglement. In Sec. III, we introduce a new scheme for creating Greenberger-Horne-Zeilinger (GHZ) [12] energy-time states and test Mermin's tripartite Bell inequality without the problem previous proposals have. In Sec. IV, we extend the scheme to create three-qutrit energy-time entangled states and then generalize the setup to prepare  $N$ -quNit energy-time entangled states of the form  $(\sum_{i=1}^N |i \dots i\rangle)/\sqrt{N}$ . In Sec. V, we discuss the sources required for generating simultaneously  $N$  particles with an unknowable time of emission and discuss some problems appearing when  $N > 2$ . Finally, in Sec. VI, we present our conclusions.

## II. FRANSON-LIKE CONFIGURATIONS ARE INADEQUATE FOR MULTIPARTITE BELL EXPERIMENTS

Franson-like configurations for  $N = 3$  and  $N = 4$  particles have been proposed in Refs. [13,14]. The simplest case,  $n = 3$ , is illustrated in Fig. 1. In these configurations, each of the  $n$  parties is at the end of an interferometer with a short path  $S$  and a long path  $L$ , and particle  $i$  always ends in party  $P_i$ 's detectors. Similar configurations can be easily constructed for  $N \geq 3$  parties by adding more arms [13,14]. In this section we assume that we have a source emitting simultaneously three particles

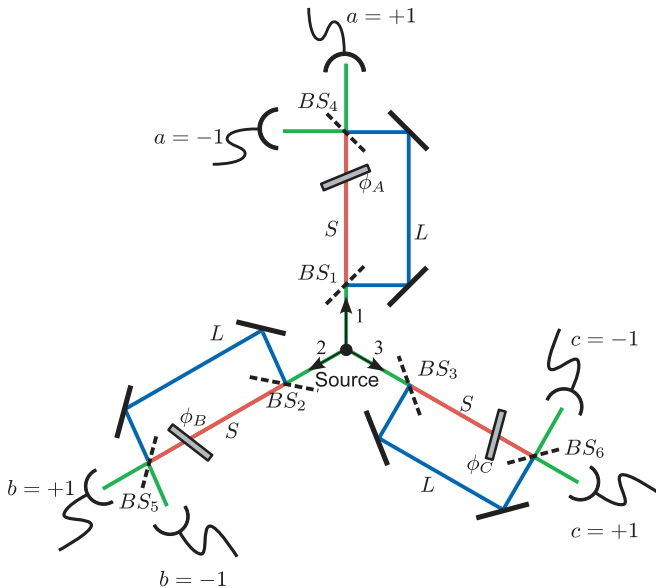


FIG. 1. (Color online) Setup for a Franson-like energy-time three-party GHZ experiment. The source emits three particles (1, 2, and 3) at the same unknown time. Each of them is fed into an unbalanced interferometer with a short ( $S$ ) and a long ( $L$ ) path. The essential uncertainty in the time of emission makes undistinguishable the case where the three photons are detected at time  $t_0$  after the time of emission ( $SSS$ ) from the case where the three photons are detected at time  $t_1 = t_0 + \Delta t$  after the time of emission ( $LLL$ ).

at an unknown time (actual sources with approximately this property will be discussed in Sec. V).

The setup in Fig. 1 is inadequate for testing the three-party Bell-Mermin inequality [11] inspired by GHZ proof of quantum nonlocality [12]. The three-party Bell-Mermin inequality is

$$\mu := |\langle A_0 B_0 C_1 \rangle + \langle A_0 B_1 C_0 \rangle + \langle A_1 B_0 C_0 \rangle - \langle A_1 B_1 C_1 \rangle| \leq 2, \quad (1)$$

where  $A_0$  and  $A_1$  are dichotomic observables with possible values  $+1$  or  $-1$  on Alice's qubit,  $B_0$  and  $B_1$  are dichotomic observables on Bob's qubit, and  $C_0$  and  $C_1$  are dichotomic observables on Carol's qubit.

According to quantum mechanics, the largest violation of inequality (1) is obtained by preparing the GHZ state

$$|\text{GHZ}\rangle = \frac{1}{\sqrt{2}}(|SSS\rangle + |LLL\rangle), \quad (2)$$

which is an eigenstate with eigenvalue  $-1$  of  $\sigma_x^{(1)} \otimes \sigma_y^{(2)} \otimes \sigma_y^{(3)}$ ,  $\sigma_y^{(1)} \otimes \sigma_x^{(2)} \otimes \sigma_y^{(3)}$ ,  $\sigma_y^{(1)} \otimes \sigma_y^{(2)} \otimes \sigma_x^{(3)}$ , and  $-\sigma_x^{(1)} \otimes \sigma_x^{(2)} \otimes \sigma_x^{(3)}$ , and measuring the following six local observables:

$$A_0 = \sigma_y^{(1)}, \quad A_1 = \sigma_x^{(1)}, \quad (3a)$$

$$B_0 = \sigma_y^{(2)}, \quad B_1 = \sigma_x^{(2)}, \quad (3b)$$

$$C_0 = \sigma_y^{(3)}, \quad C_1 = \sigma_x^{(3)}, \quad (3c)$$

Then, quantum mechanics predicts  $\mu = 4$ , which maximally violates inequality (1).

The setup of Fig. 1 can be used to produce the GHZ state (2) by postselecting threefold coincidences (i.e., those events in which all three photons are detected at the same time). This occurs in 25% of the cases. In the other cases, with equal frequencies, either two photons are detected at time  $t_0$  and one photon is detected at time  $t_1 = t_0 + \Delta t$  or one photon is detected at time  $t_0$  and two photons are detected at time  $t_1$ . The parties must store the coincident events and reject the other events.

However, Table I shows a local HV model which reproduces the quantum predictions and, in particular, gives  $\mu = 4$ . In the model, for each local measurement, the outcomes  $S+$  (denoting that the photon will be detected at time  $t_0$  in the detector  $+1$ ),  $S-$ ,  $L+$ , and  $L-$  (denoting that the photon will be detected at time  $t_1$  in the detector  $-1$ ) are obtained with equal probability (as predicted by quantum mechanics). Three-fourths of the events are rejected during the postselection procedure because in that cases not all three photons are detected. For the selected events,  $\mu = 4$ , which is the violation predicted by quantum mechanics for an ideal experiment. Actually, similar local HV models can be constructed to simulate any value  $\mu \leq 4$ . Moreover, similar local HV models can be constructed to simulate any quantum prediction for any  $N$ -party Mermin inequality using a Franson-like configuration like the one in Fig. 1, but with an arbitrary number  $N \geq 2$  of parties, each of them with two settings.

## III. PROPOSED TEST OF MERMIN INEQUALITY WITH THREE-QUBIT GHZ ENERGY-TIME STATES

The setups in Refs. [13,14] cannot exclude local HV models like the one introduced in the previous section. Then, a

TABLE I. 1536 sets of instructions of the local HV model. Each row represents 96 sets of local instructions (first six entries) and their corresponding contributions for the calculation of  $\mu$  after applying the postselection procedure (last four entries). In the first row,  $L, L, L/S$  denotes the 48 sets with three  $L$  or two  $L$  and one  $S$ , with all possible combinations of signs:  $L+, L+, L+; L+, L+, S+; L+, S+, L+; \dots; S-, L-, L-$ . The other 48 sets are obtained by interchanging  $S$  and  $L$ .

$A_0$	$A_1$	$B_0$	$B_1$	$C_0$	$C_1$	$\langle A_0 B_0 C_1 \rangle$	$\langle A_0 B_1 C_0 \rangle$	$\langle A_1 B_0 C_0 \rangle$	$\langle A_1 B_1 C_1 \rangle$
$S+$	$L$	$S+$	$L$	$L/S$	$S+$	+1	Rejected	Rejected	Rejected
$S+$	$L$	$S-$	$L$	$L/S$	$S-$	+1	Rejected	Rejected	Rejected
$S-$	$L$	$S+$	$L$	$L/S$	$S-$	+1	Rejected	Rejected	Rejected
$S-$	$L$	$S-$	$L$	$L/S$	$S+$	+1	Rejected	Rejected	Rejected
$S+$	$L$	$L$	$S+$	$S+$	$L/S$	Rejected	+1	Rejected	Rejected
$S+$	$L$	$L$	$S-$	$S-$	$L/S$	Rejected	+1	Rejected	Rejected
$S-$	$L$	$L$	$S+$	$S-$	$L/S$	Rejected	+1	Rejected	Rejected
$S-$	$L$	$L$	$S-$	$S+$	$L/S$	Rejected	+1	Rejected	Rejected
$L$	$S+$	$S+$	$L$	$S+$	$L/S$	Rejected	Rejected	+1	Rejected
$L$	$S+$	$S-$	$L$	$S-$	$L/S$	Rejected	Rejected	+1	Rejected
$L$	$S-$	$S+$	$L$	$S-$	$L/S$	Rejected	Rejected	+1	Rejected
$L$	$S-$	$S-$	$L$	$S+$	$L/S$	Rejected	Rejected	+1	Rejected
$L$	$S+$	$L$	$S+$	$L/S$	$S-$	Rejected	Rejected	Rejected	-1
$L$	$S+$	$L$	$S-$	$L/S$	$S+$	Rejected	Rejected	Rejected	-1
$L$	$S-$	$L$	$S+$	$L/S$	$S+$	Rejected	Rejected	Rejected	-1
$L$	$S-$	$L$	$S-$	$L/S$	$S-$	Rejected	Rejected	Rejected	-1

natural question is how to exclude them and perform a genuine test the Mermin inequality with energy-time entanglement. In this section we provide a solution based on a new configuration which is a natural extension to three or more parties of the scheme introduced in Ref. [5]. The advantage over the set up in Fig. 1 discussed in Sec. II is that, in the case of perfect detectors, with the new configuration the expected results cannot be simulated with any local HV model.

The crucial difference between the setups of Figs. 1 and 2 is that while the geometry of the set up in Fig. 1 does not prevent that the selection and rejection of events can be affected by the local phase settings, the geometry of the setup in Fig. 2 prevents this possibility. Therefore, while in local HV models for experiments using the setup of Fig. 1 the decision of being detected or not can depend on the local setting, in any local HV model for experiments using the setup of Fig. 2, the fact that the photon is detected or not must be independent of the local phase settings; and there are no such local HV models reproducing the quantum predictions.

To illustrate this difference, first consider a selected event: the three photons have been detected at time  $t_0$  (or at time  $t_1$ ). Although the phase setting of  $\phi_A$ ,  $\phi_B$ , and  $\phi_C$  are, respectively, in the backward light cones of the photons detected in Alice, Bob, and Carol's sides, as in the setup of Fig. 1, the key point is that, in Fig. 2, different values of the phase settings cannot cause a selected event to become a rejected event, since this would require a mechanism to make one detection to "wait" until the information about the setting in other side comes. However, when this information has finally arrived, the phase settings (both of them) have changed, so this information is useless to base a decision on it.

On the contrary, for the setup of Fig. 2, there is no physical mechanism preserving locality which can turn a selected (rejected) event into a rejected (selected) event. The selected events are independent of the local phase settings. For the selected events, only the +1 or -1 decision can depend on the phase settings. This is exactly the assumption under which

the Mermin inequality (1) and their generalizations to  $N > 3$  parties are valid. Therefore, an experimental violation of (1) using the setup of Fig. 2 and the postselection procedure described before provides a conclusive (assuming perfect detectors) test of local realism using energy-time (or time-bin) entanglement.

#### IV. GENERATION OF $N$ -qubit ENERGY-TIME ENTANGLED STATES

##### A. Three-qutrit energy-time entangled states

An interesting feature of the setup in Fig. 2 is that it can be extended to prepare  $N$ -qubit energy-time entangled states with potential applications in quantum information processing.

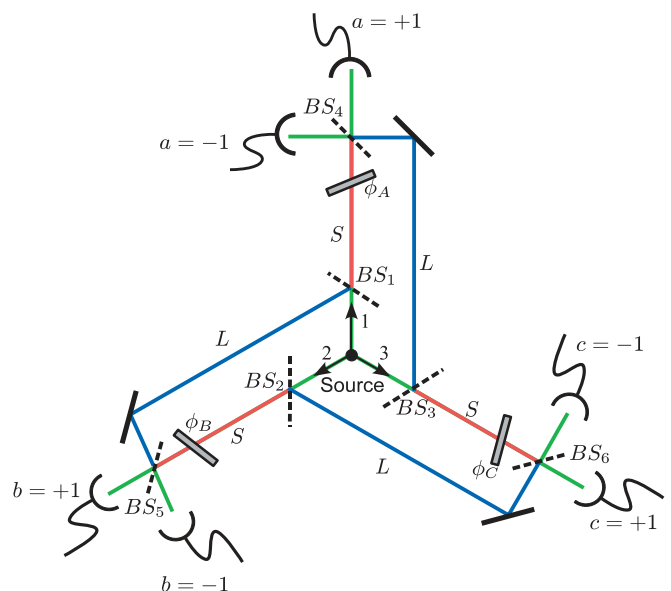


FIG. 2. (Color online) Setup for preparing a three-qubit energy-time GHZ state. All the beam splitters (BSs) are 50/50 BSs.

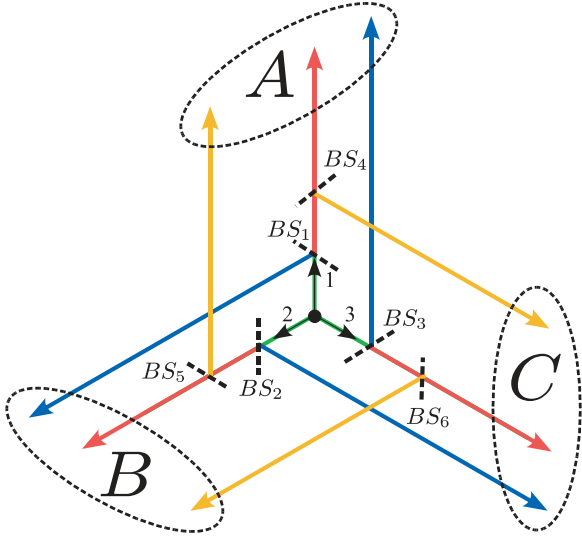


FIG. 3. (Color online) Setup for preparing the state (4).  $BS_1, BS_2, BS_3$  have reflection coefficient  $R = \frac{1}{3}$ , while  $BS_4, BS_5, BS_6$  have  $R = \frac{1}{2}$ .

For instance, using the setup shown in Fig. 3, we can prepare the three-qutrit state

$$|\Psi\rangle = \frac{1}{\sqrt{3}}(|111\rangle + |222\rangle + |333\rangle) \quad (4)$$

by using a source emitting three photons simultaneously at an unknown time and then postselecting the threefold coincidences. The geometry of the setup is suitable for three-qutrit Bell tests (i.e., is free of the problems discussed in Sec. III).

The setup for performing one observer's local measurements is shown in Fig. 4. The three BSs in Fig. 4, written in the basis  $|1\rangle, |2\rangle, |3\rangle$ , are given by

$$BS_1^A = \begin{pmatrix} 1 & 0 & 0 \\ 0 & \frac{1}{\sqrt{2}} & \frac{e^{i\alpha}}{\sqrt{2}} \\ 0 & \frac{1}{\sqrt{2}} & -\frac{e^{i\alpha}}{\sqrt{2}} \end{pmatrix}, \quad (5a)$$

$$BS_2^A = \begin{pmatrix} \frac{\sqrt{2}}{\sqrt{3}} & 0 & \frac{e^{i\beta}}{\sqrt{3}} \\ 0 & 1 & 0 \\ \frac{1}{\sqrt{3}} & 0 & -\frac{\sqrt{2}e^{i\beta}}{\sqrt{3}} \end{pmatrix}, \quad (5b)$$

$$BS_3^A = \begin{pmatrix} \frac{1}{\sqrt{2}} & \frac{e^{i\gamma}}{\sqrt{2}} & 0 \\ \frac{1}{\sqrt{2}} & -\frac{e^{i\gamma}}{\sqrt{2}} & 0 \\ 0 & 0 & 1 \end{pmatrix}. \quad (5c)$$

Therefore,  $BS_1^A$  and  $BS_3^A$  are 50-50 BSs, while  $BS_2^A$  has a reflection coefficient  $R = \frac{1}{3}$ . The action of the three BSs in Fig. 4 corresponds to the following unitary operator:

$$M := BS_3^A BS_2^A BS_1^A = \frac{1}{\sqrt{3}} \begin{pmatrix} 1 & \frac{\sqrt{3}e^{i\gamma} + e^{i\beta}}{2} & \frac{1}{2}e^{i\alpha}(\sqrt{3}e^{i\gamma} - e^{i\beta}) \\ 1 & \frac{-\sqrt{3}e^{i\gamma} + e^{i\beta}}{2} & -\frac{1}{2}e^{i\alpha}(\sqrt{3}e^{i\gamma} + e^{i\beta}) \\ 1 & -e^{i\beta} & e^{i(\beta+\alpha)} \end{pmatrix}. \quad (6)$$

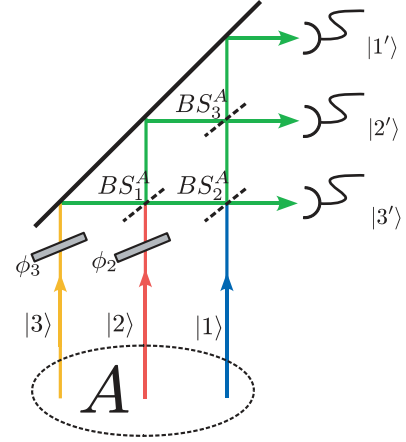


FIG. 4. (Color online) Setup for the measurement of a qutrit state. The reflection coefficients are given in (5a)–(5c).

By choosing  $\beta = \frac{\pi}{3}$ ,  $\gamma = -\frac{\pi}{6}$  and  $\alpha = \pi/3$ , we obtain

$$M = \frac{1}{\sqrt{3}} \begin{pmatrix} 1 & 1 & 1 \\ 1 & e^{i\frac{2\pi}{3}} & e^{i\frac{4\pi}{3}} \\ 1 & e^{i\frac{4\pi}{3}} & e^{i\frac{8\pi}{3}} \end{pmatrix}. \quad (7)$$

By inserting the three phases  $\phi_i$ , we obtain

$$M = \frac{1}{\sqrt{3}} \begin{pmatrix} 1 & e^{-i\phi_2} & e^{-i\phi_3} \\ 1 & e^{i\frac{2\pi}{3}}e^{-i\phi_2} & e^{i\frac{4\pi}{3}}e^{-i\phi_3} \\ 1 & e^{i\frac{4\pi}{3}}e^{-i\phi_2} & e^{i\frac{8\pi}{3}}e^{-i\phi_3} \end{pmatrix}. \quad (8)$$

This measurement projects onto the basis

$$|1'\rangle = M^\dagger|1\rangle, \quad |2'\rangle = M^\dagger|2\rangle, \quad |3'\rangle = M^\dagger|3\rangle, \quad (9)$$

given by

$$|1'\rangle = \frac{1}{\sqrt{3}}(|1\rangle + e^{i\phi_2}|2\rangle + e^{i\phi_3}|3\rangle), \quad (10a)$$

$$|2'\rangle = \frac{1}{\sqrt{3}}(|1\rangle + e^{i(\phi_2 - \frac{2\pi}{3})}|2\rangle + e^{i(\phi_3 - \frac{4\pi}{3})}|3\rangle), \quad (10b)$$

$$|3'\rangle = \frac{1}{\sqrt{3}}(|1\rangle + e^{i(\phi_2 - \frac{4\pi}{3})}|2\rangle + e^{i(\phi_3 - \frac{2\pi}{3})}|3\rangle). \quad (10c)$$

## B. Generalization to $N$ quNits

Interestingly, the setup can be extended to prepare  $N$ -quNit energy-time entangled states with  $N > 3$ . For each particle we use a scheme given in Fig. 5 to generate a quNit. Each mode is sent to a different party  $A_i$ . Then, by using a scheme similar to that proposed in Refs. [15,16] we can measure the quNit.

The BSs described in Fig. 6 can be set to produce the following unitary transformation

$$\mathcal{U} = \frac{1}{\sqrt{N}} \begin{pmatrix} 1 & 1 & 1 & \dots & 1 \\ 1 & \omega & \omega^2 & \dots & \omega^{N-1} \\ 1 & \omega^2 & \omega^4 & \dots & \omega^{2(N-1)} \\ \vdots & \vdots & \vdots & \ddots & \vdots \\ 1 & \omega^{N-1} & \omega^{2(N-1)} & \dots & \omega^{(N-1)^2} \end{pmatrix}, \quad (11)$$

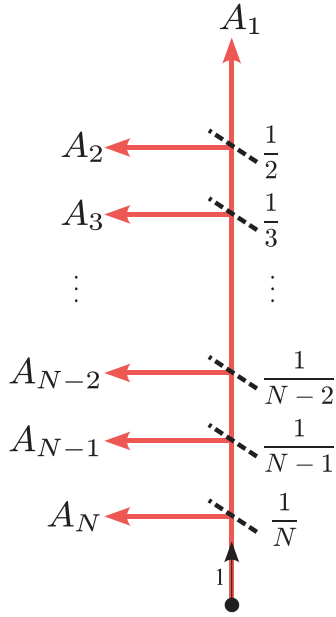


FIG. 5. (Color online) Generation of  $N$ -particle  $qN/it$  state. The reflection coefficients are shown on the right side of the corresponding BS.

where

$$\omega = e^{\frac{2\pi i}{N}}. \quad (12)$$

We have

$$\mathcal{U}_{ij} = \omega^{(i-1)(j-1)}. \quad (13)$$

With the phase shift we measure on the following basis:

$$|1'\rangle = \frac{1}{\sqrt{N}}(|1\rangle + e^{i\phi_2}|2\rangle + \dots + e^{i\phi_N}|N\rangle), \quad (14a)$$

$$|2'\rangle = \frac{1}{\sqrt{N}}(|1\rangle + \bar{\omega}e^{i\phi_2}|2\rangle + \dots + \bar{\omega}^{N-1}e^{i\phi_N}|N\rangle), \quad (14b)$$

$$|3'\rangle = \frac{1}{\sqrt{N}}(|1\rangle + \bar{\omega}^2e^{i\phi_2}|2\rangle + \dots + \bar{\omega}^{2(N-1)}e^{i\phi_N}|N\rangle), \dots, \quad (14c)$$

$$|N'\rangle = \frac{1}{\sqrt{N}}(|1\rangle + \bar{\omega}^{N-1}e^{i\phi_2}|2\rangle + \dots + \bar{\omega}^{(N-1)^2}e^{i\phi_N}|N\rangle). \quad (14d)$$

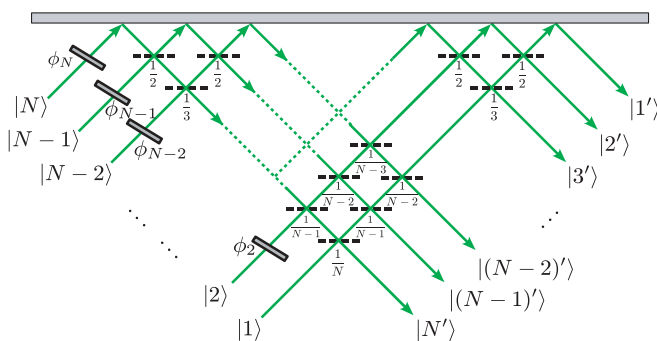


FIG. 6. (Color online) Measurement of a  $qN/it$  state. The reflection coefficients are shown below the corresponding BS.

These states can be used for GHZ proofs of nonlocality [17,18].

## V. SOURCES WITH UNKNOWN EMISSION TIMES

So far, we have assumed that we have sources capable of emitting three or more particles at the same unknown time. However, to our knowledge, no such sources exist. This forces us to use, in actual experiments, sources in which pairs of particles are emitted at different unknown times. The use of these sources does not solve the problem described in Sec. III but makes the problem more complex to analyze. The conclusion is still the same: Franson-like Bell experiments admit local HV models reproducing the quantum predictions, even when we use these sources. The aim of this section is to show that these sources can be used with the schemes introduced in Sec. IV, and still local HV models reproducing the quantum predictions are impossible.

For instance, in order to test the Mermin inequality on three-photon GHZ state we would need a (nonexistent) source emitting three photons at the same unknown time. However, a feasible realization is the one illustrated in Fig. 7. A femtosecond pulsed laser (with very low coherence time) is injected into a Mach-Zender (MZ) interferometer before shining the nonlinear crystal, from which two independent pairs are emitted at different times. The rest of the setup is similar to the one described in Sec. IV.

If  $t_0(t_1 = t_0 + \delta t)$  are the arrival time of the short (long) arm pump pulse, where  $\delta t$  is the path difference and if the two photon pairs are (1, 2) and (3, 4), then, generated state is given by

$$|\psi\rangle = \frac{1}{2}(|t_0\rangle_1|t_0\rangle_2|t_0\rangle_3|t_0\rangle_4 + |t_1\rangle_1|t_1\rangle_2|t_1\rangle_3|t_1\rangle_4 + |t_0\rangle_1|t_0\rangle_2|t_1\rangle_3|t_1\rangle_4 + |t_1\rangle_1|t_1\rangle_2|t_0\rangle_3|t_0\rangle_4). \quad (15)$$

Note that if the four photons could be generated at the same time, we would have only the first two terms in (15). The latter two terms contribute to events that are detected on different sides and are not coincident. In order to discard them, we should shorten the coincidence windows.

Now the question is whether the selected (rejected) events could have been rejected (selected) events for a different value

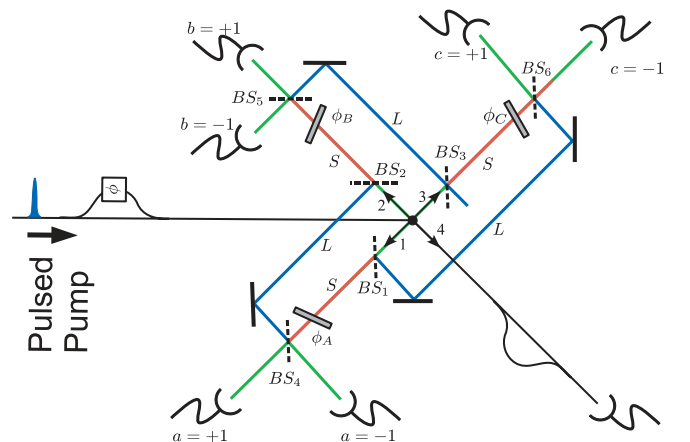


FIG. 7. (Color online) Realistic setup for a test of the three-party Mermin inequality with energy-time entangled photons.



of one of the local settings. The key point to see that this cannot happen is to remember that photons 1 and 2 (3 and 4), when the four photons arrive at four different locations, are always detected at the same time. Then, only a nonlocal mechanism can change the arrival time of *both* photons due to a different local setting in *one* of the photons. In principle, the detection of photon 1 at time  $t_0$  or  $t_1$  could depend of the local setting. The problem for any local HV model reproducing the quantum predictions is that photon 2 should be detected at the same time, and this requires nonlocal communication. Therefore, the use of these sources do not cause any fundamental problem if the detectors are perfect.

## VI. CONCLUSIONS

Franson's energy-time entanglement was a great achievement because it provided a new experimentally feasible method to generate photonic entanglement. However, the fact that (without supplementary assumptions) the outcomes of actual Bell-CHSH experiments, and even those of ideal experiments, can be reproduced with local HV models weakens the power of the idea. In a previous article [5], we proposed a way to solve this problem which has been implemented

in actual experiments. Then, a natural question is whether the same problem affects previously proposed extensions of Franson's setup to the multipartite case. It does. In this article, we have shown how to extend our previous proposal to fix the problem in the multipartite case and discussed possible applications of this extension. Specifically, we have shown that, in principle, there is no fundamental obstacle to perform experimental tests of the  $N$ -party Bell inequality ( $N \geq 3$ ) proposed by Mermin [11] with energy-time entangled photons prepared in  $N$ -qubit GHZ states and how to produce a class of  $N$ -particle  $N$ -level entangled states with potential applications in quantum information processing, using energy-time.

## ACKNOWLEDGMENTS

We thank J. Franson, J.-Å. Larsson, and M. Żukowski for useful conversations. This work was supported by the Spanish Ministry of Science and Innovation's Project No. FIS2008-05596, from the Junta de Andalucía's Excellence Project No. P06-FQM-02243, and by Finanziamento Ateneo 07 Sapienza Università di Roma.

- 
- [1] J. D. Franson, Phys. Rev. Lett. **62**, 2205 (1989).
  - [2] J. Brendel, N. Gisin, W. Tittel, and H. Zbinden, Phys. Rev. Lett. **82**, 2594 (1999).
  - [3] J. F. Clauser, M. A. Horne, A. Shimony, and R. A. Holt, Phys. Rev. Lett. **23**, 880 (1969).
  - [4] S. Aerts, P. Kwiat, J.-A. Larsson, and M. Żukowski, Phys. Rev. Lett. **86**, 1909 (2001).
  - [5] A. Cabello, A. Rossi, G. Vallone, F. De Martini, and P. Mataloni, Phys. Rev. Lett. **102**, 040401 (2009).
  - [6] J. D. Franson, Phys. Rev. A **80**, 032119 (2009).
  - [7] A. Einstein, B. Podolsky, and N. Rosen, Phys. Rev. **47**, 777 (1935).
  - [8] C. Gneiting and K. Hornberger, Phys. Rev. Lett. **101**, 260503 (2008).
  - [9] G. Lima, G. Vallone, A. Chiuri, A. Cabello, and P. Mataloni, e-print arXiv:0912.4151.
  - [10] D. Frustaglia and A. Cabello, Phys. Rev. B **80**, 201312(R) (2009).
  - [11] N. D. Mermin, Phys. Rev. Lett. **65**, 1838 (1990).
  - [12] D. M. Greenberger, M. A. Horne, and A. Zeilinger, in *Bell's Theorem, Quantum Theory, and Conceptions of the Universe*, edited by M. Kafatos (Kluwer Academic, Dordrecht, Holland, 1989), p. 69.
  - [13] Y. Shih and M. Rubin, Phys. Lett. **A182**, 16 (1993).
  - [14] T. Pittman, Y. Shih, D. Strekalov, A. Sergienko, and M. Rubin, in *4th Int. Conf. on Squeezed States and Uncertainty Relations (Taiyuan, Shanxi, China, 1995)*, edited by D. Han, K. Peng, Y. Kim, and V. Man'ko (NASA, Greenbelt, Maryland, 1996), p. 139.
  - [15] M. Reck, A. Zeilinger, H. J. Bernstein, and P. Bertani, Phys. Rev. Lett. **73**, 58 (1994).
  - [16] M. Żukowski, A. Zeilinger, and M. A. Horne, Phys. Rev. A **55**, 2564 (1997).
  - [17] M. Żukowski and D. Kaszlikowski, Phys. Rev. A **59**, 3200 (1999).
  - [18] D. Kaszlikowski and M. Żukowski, Phys. Rev. A **66**, 042107 (2002).